Int. J. Heat Mass Transfer. Vol. 11, pp. 1597–1610. Pergamon Press 1968. Printed in Great Britain

SEPARATION OF GAS MIXTURE IN AN AXISYMMETRIC SUPERSONIC JET

HISASHI MIKAMI† and YOICHI TAKASHIMA‡

The Research Laboratory of Nuclear Reactor, Tokyo Institute of Technology, Tokyo, Japan

(*Received February* 1968)

Abstract—The separation of gas mixture in an axially symmetric supersonic jet is investigated.

The supersonic jet is separated into the peripheral stream and the core stream by a skimmer and the total diffusion flux of the lighter component into the peripheral stream is obtained. The experimental results are presented for the binary gas mixture of hydrogen and nitrogen.

An approximate equation is proposed which gives the diffusion flux as a function of cut and Mach number. The experimental results were in fairly good agreement with the results of calculation by the proposed equation.

NOMENCLATURE

- A, area of nozzle exit [cm^2];
- a, sonic velocity [cm/s];
- D, diameter of nozzle exit [cm];
- D_{12}, mutual diffusion coefficient [cm^2/s];
- D_T^i, thermal diffusion coefficient of species i [g/cm s];
- G, mass flow rate through nozzle [g/s];
- J_i, total mass flux of species i [g/s];
- $\mathbf{j}_i$, mass flux vector of species i [g/cm^{2}s];
- k, Boltzmann constant [erg/degK];
- N_i, mole fraction of species i [dimensionless];
- n_i, number density of species i [n/cm^3];
- M, local Mach number [dimensionless];
- M_i, molecular weight of species i [g/mol];
- M^*, critical Mach number [dimensionless];
- M^{**}, reduced molecular weight, $2M_1M_2/(M_1 + M_2)$ [g/mol];
- m_i, mass of species i [g];
- $\overline{m}$, average mass of gas mixture [g];
- P, pressure [dyn/cm^2];
- Pe, Péclet number, R^*a/D [dimensionless];
- Q_i^0, molar flow rate of species i through nozzle [mol/s];
- Q_i^M, molar flow rate of species i of peripheral stream [mol/s];
- Q_i^K, molar flow rate of species i of core stream [mol/s];
- q, numerical value of gas velocity [cm/s];
- R, universal gas constant [erg/degK mol];
- R^*, radius of nozzle exit [cm];
- Re, Reynolds number, $W\,D/\nu^\circ$ [dimensionless];
- r, distance from jet axis [cm];
- $\bar{r}$, r/R^* [dimensionless];
- St, Stanton number, $J_1/\overline{m}^0Q^0$ [dimensionless];
- s, coordinate along stream line [cm];
- T, absolute temperature [degK];
- T^*, reduced temperature, $T/(\varepsilon_{12}/k)$ [dimensionless];
- W, characteristic velocity, $\sqrt{p^0/\rho^0}$ [cm/s];
- x, distance along jet axis [cm];
- $\bar{x}$, x/R^* [dimensionless].

Greek symbols

- α, separation coefficient, $(N_1^M/N_2^M)/(N_1^0/N_2^0)$ [dimensionless];

† Associate Professor.

‡ Professor, Dr. (Engineering).

β, $1/\tan \mu$ [dimensionless];
Γ, discharge coefficient [dimensionless];
γ, ratio of specific heats [dimensionless];
ε_{12}, potential parameter for interaction between molecules 1 and 2 [erg];
ζ, $\tan \theta$ [dimensionless];
η, coordinate in characteristic coordinate system [cm];
Θ, cut [dimensionless];
θ, inclination of velocity vector [rad];
κ, curvature [cm^{-1}];
κ, $\gamma - 1/\gamma + 1$ [dimensionless];
Λ, Prandtl–Meyer function [rad];
μ, Mach angle, $\sin^{-1} 1/M$ [rad];
ν, kinematic viscosity [cm^2/s];
$\boldsymbol{\nu}$, unit vector normal to surface element $d\Sigma$ [dimensionless];
ξ, coordinate in characteristic coordinate system [cm];
ρ, density [g/cm^3];
$d\Sigma$, surface element [cm^2];
σ_{12}, collision diameter [Å];
ψ, stream function [dimensionless];
$\Omega^{(1,1)*}$, collision integral, $\Omega^{(1,1)}/\Omega^{\text{rig. sph}}$ [dimensionless].

Superscript 0 denotes the quantity at upstream condition and subscript 12 denotes the quantity for the lighter component and heavier component, respectively.

INTRODUCTION

MANY studies have been made of diffusive separation of gas mixture in a supersonic jet [1–7].

In a recent article [8], Sherman has made an analytical study on the separation of a binary gas mixture in an axially symmetric free jet and has given an equation for the mole fraction along the jet axis. Very recently, Rothe [9] showed significant experimental data on the separation of helium–argon mixtures by means of electron beam density probe and the separation results on the axis of the free jet were in fairly good agreement with Sherman's theory. Abuaf *et al.* [10] also made measurements of diffusive separation of argon–helium mixtures in free jet and there was reasonable agreement between the experimental results on the jet axis and Sherman's theory.

This paper presents the off-axis results of experiments on the separation of hydrogen and nitrogen mixture and also presents its numerical analysis. The results of numerical calculation are in fairly good agreement with the experimental results.

EXPERIMENTAL METHOD

The experiments were carried out by using the apparatus consisting of a convergent nozzle and a skimmer which were similar to those of Waterman *et al.* [3]. Details of this system are shown in Fig. 1. The nozzle and the skimmer used in this experiment are 0·3 mm and 2 mm in diameter, respectively. The distance between the nozzle exit and the skimmer can be varied by means of a micrometer screw and measured by a dial gauge to an accuracy of the order of 0·01 mm. The nozzle and the skimmer are so arranged that their centers are on a line with the aid of a travelling microscope. A flow diagram of the experimental apparatus is illustrated in Fig. 2. A binary gas mixture of known concentration was introduced to the nozzle at the inlet pressure P^0 through a needle valve and ejected at the nozzle exit at mass flow rate G. The supersonic jet thus created was separated into the peripheral stream ΘG and the central stream $(1 - \Theta)G$ by a skimmer and were pumped away by the mechanical boosters and rotary vacuum pumps, at the static pressure of P^M and P^K, respectively. The pressures P^0, P^M and P^K were measured by a di-octylphtalate oil manometer to an accuracy of the order of 0·01 mmHg. The volume flow rate of gas mixture was obtained by means of a soap film flow meter jointed to the delivery tube of the rotary vacuum pump, in which the displacement rate of a soap film meniscus in a calibrated burette was measured. A small

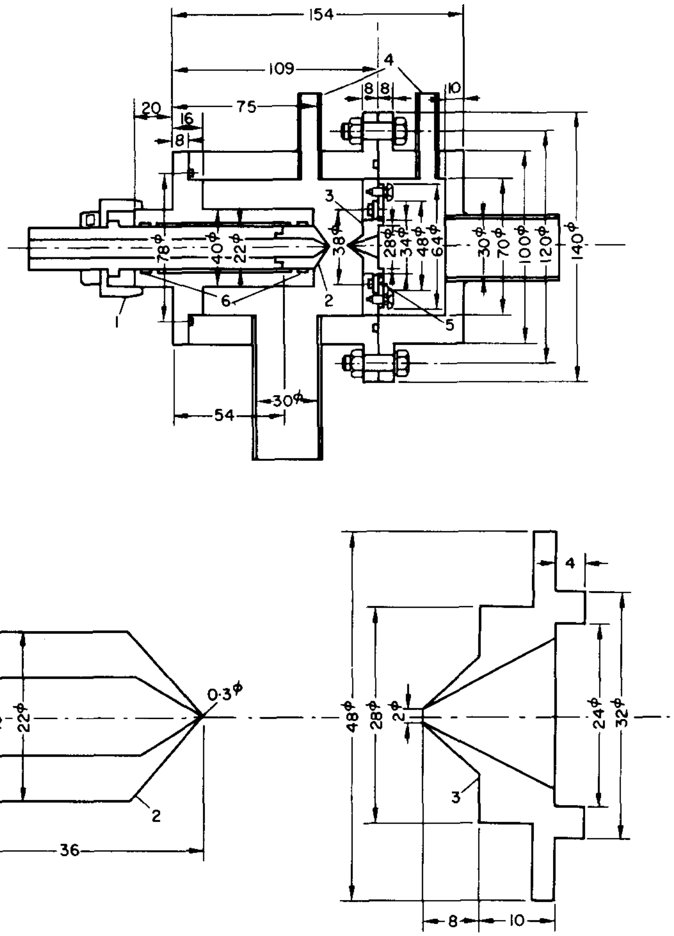

FIG. 1. Constructional details of supersonic jet apparatus. 1. Micrometer; 2. Convergent nozzle; 3. Skimmer; 4. Pressure gauge tap; 5. Flange; 6. O-ring.

amount of gas mixture was sampled from the peripheral flow into a sample bulb after slight compression by the mechanical booster. The flow of gas was maintained for about 15 min prior to sampling in order to attain a steady-state condition. The sample bulb was evacuated by a mercury diffusion pump to a pressure of about 10^{-5} mmHg before sampling. The flow rate and the concentration were measured for the peripheral stream, because a preliminary test confirmed that the calculated values on the basis of mass balance agree very well with the experimental values. The composition of the gas mixture employed in this experiment is as follows: H_2—48·92 mol%, N_2—51·08 mol%. The concentration of gas mixture at low pressure was determined to an accuracy of about 0·1 per cent by applying the low pressure constant volume method [11]. The diagram of the gas analysis apparatus is shown in Fig. 3. The gas mixture was circulated through a heated column packed with copper oxide by a mercury diffusion pump after the pressure and the gas volume were measured. Water vapour produced by the reaction of H_2 with copper oxide was removed by the liquid nitrogen trap. Non-reacting gas (N_2) was compressed to the original volume by a Töpler pump. Thus,

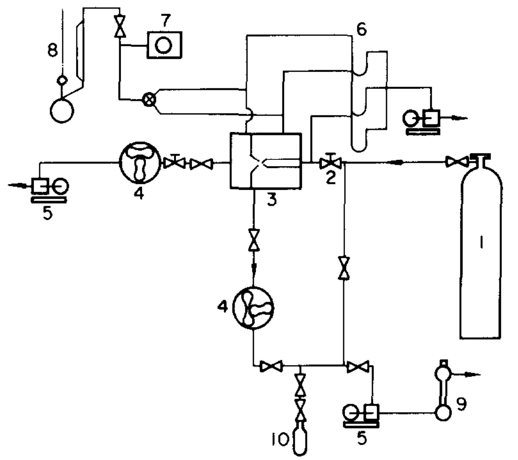

FIG. 2. Flow diagram of experimental equipment. 1. Gas mixture container; 2. Needle valve; 3. Supersonic jet apparatus; 4. Mechanical booster; 5. Rotary vacuum pump; 6. D.O.P. oil manometer; 7. Pirani gauge; 8. Macleod gauge; 9. Soap film flow meter; 10. Sample bulb.

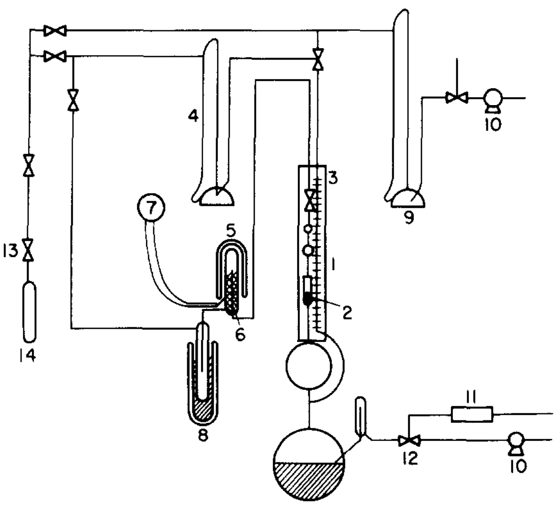

FIG. 3. Schematic diagram of gas analysis apparatus. 1. Töpler pump; 2. Mercury cut-off; 3. Glass scale; 4. Mercury diffusion pump for circulating gas mixture; 5. Nichrome wire heater; 6. Copper oxide; 7. Thermocouple; 8. Liquid nitrogen trap; 9. Mercury diffusion pump; 10. Rotary vacuum pump; 11. Silica-gel packed column; 12. Three way cock; 13. Universal joint; 14. Sample bulb.

the concentration could be determined by reading the pressure. However, the time was required over 90 min for determining the concentration of each sample. At the present time, the thermal conductivity method is being applied successfully to gas analysis at low pressure to shorten the time required in the measurement and to obtain better accuracy [12, 13].

EXPERIMENTAL RESULTS

Figure 4 shows the experimental values of volume flow rate through the nozzle as a function of inlet pressure. The ratio of downstream pressure to inlet pressure Pe/P^0 is very small and the downstream condition ceases to influence the upstream condition. The discharge coefficient Γ are calculated from these data and plotted as a function of Reynolds number in Fig. 5 where Γ and Re are defined by the following expressions.

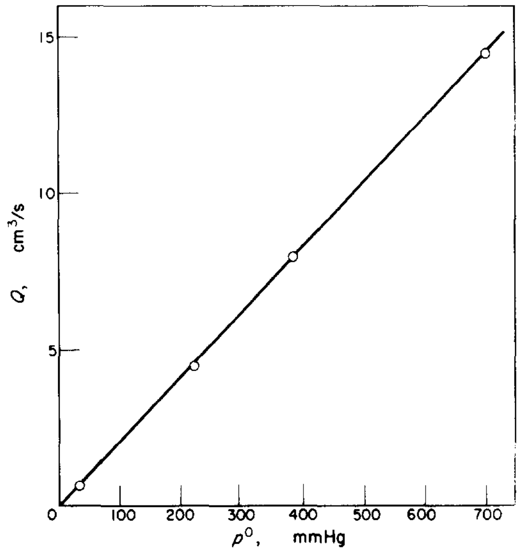

FIG. 4. Volume flow rate through nozzle versus inlet pressure.

$$G = \Gamma \rho^0 WA \tag{1}$$

$$Re = \frac{WD}{\nu^0} \tag{2}$$

$$W = \left(\frac{p^0}{\rho^0}\right). \tag{3}$$

The details of the critical mass flow of rarefied gas through nozzle are described in our report [14].

The cut Θ which means the ratio of the mass flow rate of the peripheral stream to the total mass flow rate through the nozzle is given in Fig. 6. It becomes evident that same supersonic profiles are formed for this range of inlet pressure.

In Fig. 7, the experimental data of separation coefficients are shown as a function of the distance between the nozzle exit and the skimmer with the inlet pressure as a parameter.

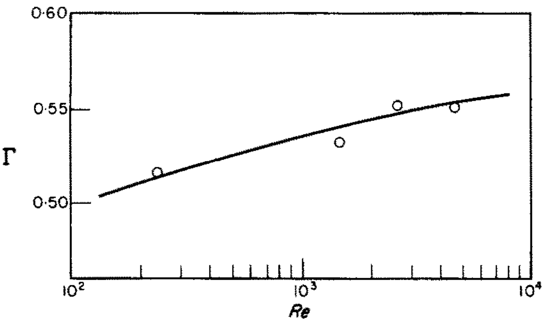

FIG. 5. Relationship between discharge coefficient and Reynolds number.

THEORETICAL ANALYSIS

As shown in Fig. 7, the lighter component (hydrogen) is enriched in the peripheral stream. This can be explained qualitatively by the fact that a large pressure gradient created in a jet causes a pressure diffusion of a lighter component in the radial direction.

The mass flux of a lighter component $\mathbf{j}_1$ relative to the center of gravity motion of gas mixture is given from the kinetic theory of gases as follows [15]:

$$\mathbf{j}_1 = \frac{n^2}{\rho} m_1 m_2 D_{12} \left\{ \operatorname{grad} N_1 - \frac{\Delta m}{\bar{m}} N_1 N_2 \operatorname{grad} \ln p \right\} - D_1^T \operatorname{grad} \ln T. \quad (4)$$

If the first term of ordinary diffusion and the third term of thermal diffusion are neglected because of a relatively small variation of concentration in space and very small value of thermal diffusion coefficient, the mass flux $\mathbf{j}_1$ is expressed as

$$\mathbf{j}_1 = -\frac{n^2}{\rho} m_1 m_2 D_{12} \frac{\Delta m}{\bar{m}} N_1 N_2 \frac{1}{p} \operatorname{grad} p. \quad (5)$$

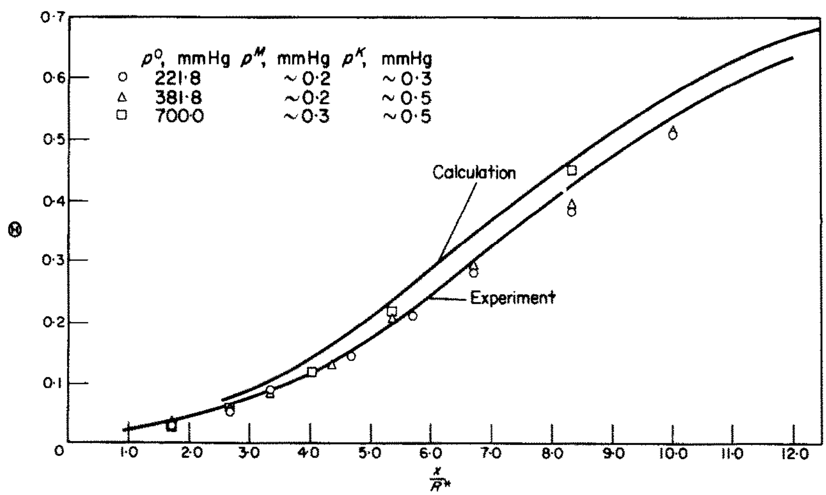

FIG. 6. Cut as a function of distance between nozzle exit and skimmer.

The total mass flux into the peripheral stream, J_1 can be obtained by integrating $\mathbf{j}_1 \cdot \mathbf{v} d\Sigma$ from the nozzle exit to the skimmer over the border surface between the peripheral and the core stream, where $\mathbf{v}$ denotes the unit vector normal to the surface element (see Fig. 8).

Thus J_1 becomes

$$J_1 = -\int_0^s \frac{n^2}{\rho} m_1 m_2 D_{12} \frac{\Delta m}{m} N_1 N_2 \frac{1}{p}\,\mathrm{grad}\, p \cdot \mathbf{v} 2\pi r\, \mathrm{d}s. \qquad (6)$$

The mutual diffusion coefficient, D_{12} is given by [16]

$$D_{12} = 2{\cdot}66\,2 \cdot 10^3 \frac{\sqrt{(T^3/M^{**})}}{p\sigma^2 \Omega^{(1,1)*}}(T^*) \qquad (7)$$

When the modified Buckingham potential is assumed for the intermolecular force, the collision integral, $\Omega^{(1\cdot1)*}$ may be approximate as

$$\Omega^{(1\cdot1)*} \simeq \mathrm{const}\, T^{*-\frac{1}{3}} \qquad (8)$$

as the calculated values of $T^{*\frac{1}{3}}\, \Omega^{(1\cdot1)*}(T^*)$ by Hirshfelder *et al.* [17] are approximately constant over a fairly wide range of T^* as shown in Fig. 9. Hence, the relation between collision integral and absolute temperature is expressed as

$$\Omega^{(1\cdot1)*} = cT^{-\frac{1}{3}}. \qquad (9)$$

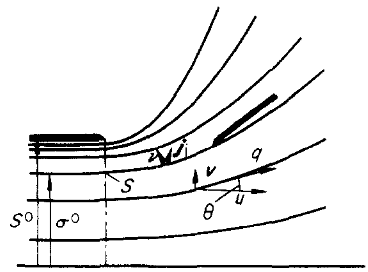

FIG. 8. Coordinates for axially symmetric flow.

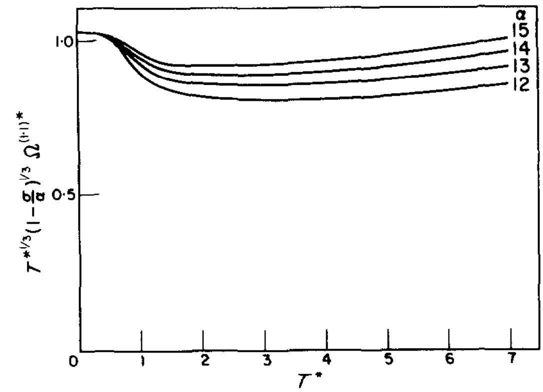

FIG. 9. Relation between collision integral and reduced temperature where α denotes potential parameter associated with the modified Buckingham potential.

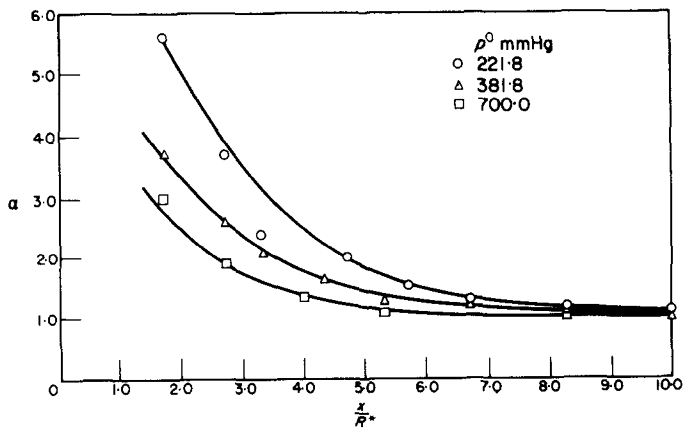

FIG. 7. Separation coefficient as a function of distance between nozzle exit and skimmer.

On the other hand, from the equation of motion in the natural coordinate system, the following expression is given

$$\operatorname{grad} p \cdot v = \kappa\rho q^2 = \frac{d\theta}{ds}\rho q^2 \qquad (10)$$

where q and θ denote the numerical value of the gas velocity and the angle of inclination of the velocity vector, respectively. By substitution of equations (9, 10) into equation (6) and with the aid of the equation of state for ideal gas, J_1 is given by

$$J_1 = \int_0^s \frac{m_1 m_2 \Delta m}{\bar{m}} N_1 N_2 \cdot 2{\cdot}662 \cdot 10^3 \sqrt{\left(\frac{M_1 + M_2}{2M_1 M_2}\right)} \frac{\sqrt{(T^3)}}{\sigma_{12}^2 C T^{-\frac{1}{3}}} \frac{q^2}{(RT)^2} \frac{d\theta}{ds} 2\pi r \, ds. \qquad (11)$$

For the convenience of calculation, a variable Λ is introduced instead of s, which is the Prandtl–Meyer function, that is,

$$\Lambda = \int_1^M \frac{\sqrt{(M^2-1)}}{1+(\gamma-1)M^2/2} \frac{dM}{M} = \sqrt{\left(\frac{\gamma+1}{\gamma-1}\right)} \tan^{-1} \sqrt{\left[\frac{\gamma-1}{\gamma+1}(M^2-1)\right]} - \tan^{-1}\sqrt{M^2-1} \qquad (12)$$

here, M represents local Mach number.

As Λ is regarded as a function of s along a streamline, equation (11) becomes

$$J_1 = \int_0^\Lambda \frac{m_1 m_2}{\bar{m}} \Delta m \, N_1 N_2 \cdot 2{\cdot}662 \cdot 10^3 \sqrt{\left(\frac{M_1 + M_2}{2M_1 M_2}\right)} \frac{\sqrt{(T^3)}}{\sigma^2 C T^{-\frac{1}{3}}} \frac{q^2}{(RT)^2} \frac{d\theta}{d\Lambda} 2\pi r \, d\Lambda. \qquad (13)$$

To reduce the above expression to nondimensional form, the following nondimensional quantities are introduced:

$$\bar{r} = \frac{r}{R^*}, \quad st = \frac{J}{\bar{m}^0 Q^0}, \quad Re = \frac{R^* a^0}{\nu^0}, \quad Sc = \frac{\nu^0}{D_{12}{}^0}, \quad M^* = \frac{q}{a^*}, \quad Pe = Re \cdot Sc$$

where a^0, ν^0, $\bar{m}^0$, D_{12}^0 and Q^0 denote the sonic velocity, the kinematic viscosity, the average mass of gas mixture, the mutual diffusion coefficient under the upstream stagnant condition and the total molar flow rate of gas mixture through the nozzle, respectively.

The Stanton number, St, is defined as the ratio of the total diffusion mass flux into the peripheral stream to the total mass flux through the nozzle. Equation (13) then reduces to

$$St = \frac{J}{\bar{m}^0 Q^0} = \frac{2\pi m_1 m_2 \Delta m D_{12}^0 n^0 a^{*2} R^* \gamma}{\bar{m}^{03} a^{02} Q^0} \int_0^\Lambda \left(\frac{T^0}{T}\right)^{\frac{1}{3}} \frac{\bar{m}^0}{\bar{m}} N_1 N_2 M^{*2} \frac{d\theta}{d\Lambda} r \, d\Lambda$$

$$= \frac{1}{Pe} \frac{2m_1 m_2 \Delta m}{\bar{m}^{03}} \gamma \left(\frac{\gamma+1}{2}\right)^{1/\gamma-1} \left(\frac{2}{\gamma+1}\right)^{\frac{1}{3}} I \qquad (14)$$

$$I = \int_0^{\Lambda} \left(\frac{T^0}{T}\right)^{\frac{1}{2}} M^{*2} \frac{d\theta}{d\Lambda} \bar{r} \frac{\bar{m}^0}{\bar{m}} N_1 N_2 \, d\Lambda. \tag{15}$$

The integral I depends approximately on both Λ and Θ. The separation coefficient α is expressed from its definition as a function of mass flux, J_1, in the following form:

$$\alpha = \frac{Q_1^M/Q_2^M}{N_1^0/N_2^0} = \frac{N_2^0 m_2}{N_1^0 m_1} \frac{m_1 N_1^0 \Theta Q^0 + J_1}{m_2 N_2^0 \Theta Q^0 - J_1} \tag{16}$$

where Q_i^M is the molar flow rate of i component of the peripheral stream. Then, from equations (14, 16) the relationship between Stanton number and separation coefficient is given by

$$St = \frac{m_1 N_1^0}{\bar{m}^0} \Theta_G \frac{\alpha - 1}{1 + \alpha \dfrac{m_1 N_1^0}{m_2 N_2^0}}. \tag{17}$$

The Péclet number is given by

$$Pe = \frac{R^* a^0}{D_{12}^0} = R^* \sqrt{\left(\gamma \frac{1}{\bar{m}^0} k T^0\right)} \frac{1}{D_{12}^0}$$

$$= R^* \sqrt{\left(\gamma \frac{1}{\bar{m}^0} k T^0\right)} \frac{1}{2{\cdot}662 \cdot 10^3 \dfrac{\sqrt{[T^3(M_1 + M_2)/2M_1 M_2]}}{p^0 \sigma_{12}^2 \Omega_{12}^{(1\cdot1)*} (T_{12}^{*0})}} \tag{18}$$

The force constants σ_{12} and ε_{12} associated with the Lennard–Jones potential for interaction between hydrogen and nitrogen molecules are found in the reference [18] to be

$$\sigma_{12} = 3{\cdot}305\,\text{Å}, \qquad \varepsilon_{12}/k = 58{\cdot}1\,°\text{K}.$$

From the experimental results for α and Θ, the value of

$$\frac{St \cdot Pe}{\dfrac{2 m_1 m_2 \Delta m}{\bar{m}^{03}} \gamma \left(\dfrac{\gamma + 1}{2}\right)^{1/\gamma - 1} \left(\dfrac{2}{\gamma + 1}\right)^{\frac{1}{2}}}$$

is calculated with the aid of equation (17, 18) and plotted as a function of nozzle to skimmer distance with the inlet pressure as a parameter in Fig. 10. It is indicated, in Fig. 10, that experimental results for various inlet pressures can be summarized with a single relation by using the above dimensionless quantities.

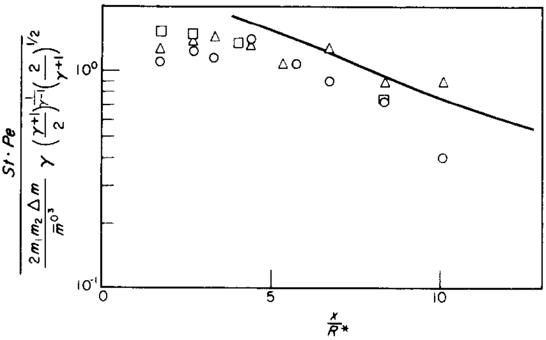

FIG. 10. Summary of the separation results.

NUMERICAL ANALYSIS

In this section, the flow field of an axially symmetric supersonic jet is computed by using the numerical method of characteristics and both $d\theta/d\Lambda$ and I which appeared in equation (14) are calculated along various streamlines.

The equations of motion in the characteristic coordinate system, are given in the following form [19]

$$\frac{\partial}{\partial \eta}(\Lambda - \theta) = \sin \mu \frac{\sin \theta}{r} \tag{19}$$

$$\frac{\partial}{\partial \xi}(\Lambda + \theta) = \sin \mu \frac{\sin \theta}{r} \tag{20}$$

where ξ and η denote coordinates and r and $\mu[= \sin^{-1}(1/M)]$ denote the distance from jet axis and Mach angle, respectively. The equations for the directions of the characteristic curves are

$$\left(\frac{dr}{dx}\right)_{\pm} = \tan(\theta \pm \mu) \tag{21}$$

and the elementary increments of characteristic curves, $d\xi$, $d\eta$ are given by

$$\left.\begin{matrix} d\xi \\ d\eta \end{matrix}\right\} = dr\sqrt{1 + \left(\frac{dx}{dr}\right)_{\pm}^{2}}. \tag{22}$$

From equations (21, 22) the equations of motion along characteristic curves become

$$d\Lambda \mp d\theta = \frac{\sin\mu \cdot \sin\theta}{r\sin(\theta \pm \mu)} dr. \tag{23}$$

In order to save the machine time of computation, new variables β and ζ have been introduced instead of Λ and θ by Chushkin [20], Katskova [21, 22], Wang and Peterson [23]. β and ζ are given by

$$\beta = \frac{1}{\tan\mu} = \sqrt{(M^2 - 1)} \tag{24}$$

$$\zeta = \tan\theta. \tag{25}$$

Then, equation (23) becomes

$$d\zeta \mp \frac{2\beta^2(1 + \zeta^2)\,d\beta}{(\gamma + 1)(1 + \beta^2)(1 + \kappa\beta^2)} \pm \frac{\zeta(1 + \zeta^2)\,dr}{(\beta\zeta \pm 1)\,r} = 0 \tag{26}$$

$$\kappa = \frac{\gamma - 1}{\gamma + 1}.$$

In equation (26), there appear no trigonometric functions which occupy a significant portion of computation time. The computing procedure used in this study is briefly described below. The familiar step by step method of characteristics was used in which the known solution at two points P_1, P_2 leads to the solution at point P_3 (see Fig. 11). The difference equations based on equation (26) are given in the following equations.

$$r_3 = \frac{r_2 - mnr_1 + n(x_1 - x_2)}{(1 - mn)} \tag{27}$$

$$x_3 = x_1 + m(r_3 - r_1) \tag{28}$$

$$\beta_3 = \frac{1}{K \cdot F + I \cdot E}\{E[I\beta_2 + F(\zeta_1 - \zeta_2) - N(x_3 - x_2)] + F(K\beta_1 - L(r_3 - r_1))]\} \tag{29}$$

$$\zeta_3 = \zeta_1 - \frac{1}{E}[K(\beta_3 - \beta_1) + L(r_3 - r_1)] \tag{30}$$

$$m = \frac{1}{2}\left(\frac{\beta_1 - \zeta_1}{\beta_1\zeta_1 + 1} + \frac{\beta_3 - \zeta_3}{\beta_3\zeta_3 + 1}\right) \tag{31}$$

$$n = \frac{1}{2}\left(\frac{\beta_2\zeta_2 - 1}{\beta_2 + \zeta_2} + \frac{\beta_3\zeta_3 - 1}{\beta_3 + \zeta_3}\right) \tag{32}$$

$$E = \frac{1}{2}\left(\frac{1}{1 + \zeta_1^2} + \frac{1}{1 + \zeta_3^2}\right) \tag{33}$$

$$F = \frac{1}{2}\left(\frac{1}{1 + \zeta_2^2} + \frac{1}{1 + \zeta_3^2}\right) \tag{34}$$

$$K = -\frac{1}{2}\left(\frac{2\beta_1^2}{(\gamma + 1)(1 + \beta_2^2)(1 + \kappa\beta_2^2)} + \frac{2\beta_3^2}{(\gamma + 1)(1 + \beta_3^2)(1 + \kappa\beta_3^2)}\right) \tag{35}$$

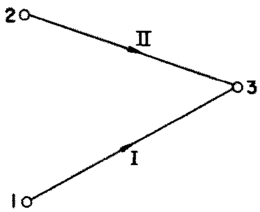

FIG. 11. Computation of unknown point 3 from two known points 1, 2.

$$I = -\frac{1}{2}\left(\frac{2\beta_2^2}{(\gamma + 1)(1 + \beta_2^2)(1 + \kappa\beta_2^2)} + \frac{2\beta_3^2}{(\gamma + 1)(1 + \beta_3^2)(1 + \kappa\beta_3^2)}\right) \tag{36}$$

$$L = \frac{1}{2}\left(\frac{\zeta_1}{(\beta_1\zeta_1 + 1)r_1} + \frac{\zeta_3}{(\beta_3\zeta_3 + 1)r_3}\right) \quad (37)$$

$$N = \frac{1}{2}\left(\frac{\zeta_2}{(\beta_2\zeta_2 + 1)r_2} + \frac{\zeta_3}{(\beta_3\zeta_3 + 1)r_3}\right). \quad (38)$$

The above formulas can be used for calculating interior point from two noncentral points. Special consideration is necessary for calculating central point.

As $r \to 0$ along a characteristic, ζ/r is given by

$$\lim_{r\to 0} \frac{\zeta}{r} = \left(\frac{d\zeta}{dr}\right)_{r=0} = \left(\frac{d\theta}{dr}\right)_{\pm,r=0} \quad (39)$$

$(d\theta/dr)_{I,r=0}$ can be obtained by making use of equation (26), which is rewritten to

$$\sec^2\theta\left(\frac{d\theta}{dr}\right)_{\pm} \mp \frac{2\beta^2(1+\zeta^2)}{(\gamma+1)(1+\beta^2)(1+\kappa\beta^2)} \left(\frac{d\beta}{dr}\right) \pm \frac{\zeta(+\zeta^2)}{(\beta\zeta \pm 1)r} = 0. \quad (40)$$

As $r \to 0$, the above equation becomes

$$\left(\frac{d\theta}{dr}\right)_{\pm} \mp \frac{2\beta^2}{(\gamma+1)(1+\beta^2)(1+\kappa\beta^2)}\left(\frac{d\beta}{dr}\right) \pm \left(\frac{d\theta}{dr}\right)_{\pm} = 0. \quad (41)$$

Then $(d\theta/dr)_{\pm,r=0}$ are given by

$$\left(\frac{d\theta}{dr}\right)_{\pm,r=0} = \frac{\beta^2}{(\gamma+1)(1+\beta^2)(1+\kappa\beta^2)} \times \left(\frac{d\beta}{dr}\right)_{r=0} \quad (42)$$

The expressions for ζ_1/r_1 and ζ_3/r_3 on the axis become

$$\frac{\zeta_1}{r_1} = \frac{\beta_1^2}{(\gamma+1)(1+\beta_1^2)(1+\kappa\beta_1^2)}\frac{\beta_3-\beta_1}{r_3} \quad (43)$$

$$\frac{\zeta_3}{r_3} = \frac{\beta_3^2}{(\gamma+1)(1+\beta_3^2)(1+\kappa\beta_3^2)}\frac{\beta_3-\beta_2}{r_2}. \quad (44)$$

It is necessary for obtaining the solution at an unknown point P_3 to use an iterative process which is started with an initial assumption for the coefficients, m, E, K, L, n, F, I, J and is continued until the criterion

$$\max\left(\left|\frac{r_3^n - r_3^{n-1}}{r_3^{n-1}}\right|, \left|\frac{x_3^n - x_3^{n-1}}{x_3^{n-1}}\right|, \left|\frac{\beta_3^n - \beta_3^{n-1}}{\beta_3^{n-1}}\right|, \left|\frac{\zeta_3^n - \zeta_3^{n-1}}{\zeta_3^{n-1}}\right|\right) \leqslant 10^{-6} \quad (45)$$

is satisfied.

The initial estimation of the coefficients m, E, K, L was made by assuming that $\zeta_3 = \zeta_1$, $\beta_3 = \beta_1$, $r_3 = r_1$, $x_3 = x_1$ and of the coefficients n, F, I, J by assuming that $\zeta_3 = \zeta_2$, $\beta_3 = \beta_2$, $r_3 = r_2$, $x_3 = x_2$.

The intial set of the data were obtained from the table presented by Katskova [20] who computed the flow field of an axially symmetric supersonic jet near the nozzle exit. The change in the stream function, ψ along a characteristics curve is given by

$$d\psi = \left(\frac{d\psi}{\partial r}\right)dr + \left(\frac{d\psi}{\partial x}\right)dx = \frac{2\rho}{\rho^*} r\,dx \left[u\left(\frac{dr}{dx}\right)_{\pm} - v\right]. \quad (46)$$

From equation (21),

$$\left(\frac{dr}{dx}\right)_{\pm} = \tan(\theta \pm \mu) = \frac{\beta\zeta \mp 1}{\beta + \zeta}. \quad (47)$$

Substitution of equation (47) into equations (46) gives

$$d\psi = -2\frac{\rho}{\rho^*} rM^* \frac{(1+\zeta^2)^{\frac{1}{2}}}{(\beta+\zeta)} dx. \quad (48)$$

Then the difference equation for ψ_3 is given by

$$\psi_3 = \psi_2 - \left(\frac{r_2\rho_2 M_2^*}{\zeta_2 + \beta_2}\sqrt{(1+\zeta_2^2)} + \frac{r_3\rho_3 M_3^*}{\zeta_3 + \beta_3}\sqrt{(1+\zeta_3^2)}\right)(x_3 - x_2). \quad (49)$$

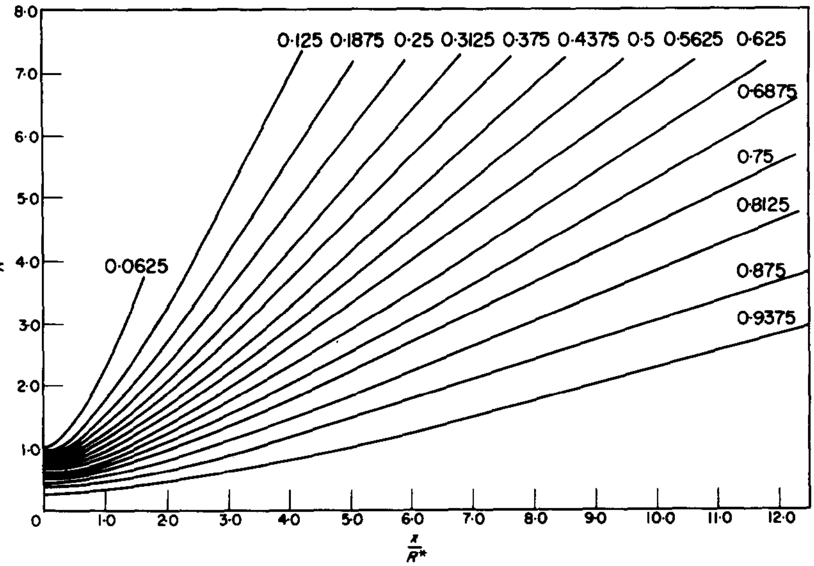

FIG. 12. Streamlines of an axisymmetric flow of a freely expanding gas.

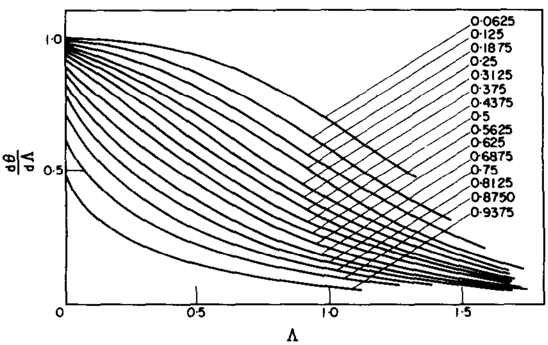

FIG. 13. $d\theta/d\Lambda$ vs. Λ for various values of cut.

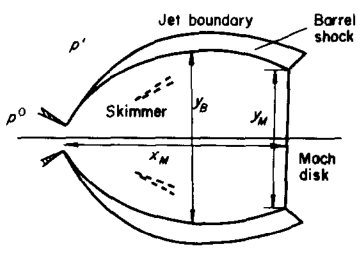

FIG. 14. Flow geometry of supersonic free jet.

The number of computed points was so determined that the increments of both x/R^* and r/R^* are maintained less than 0·02. In Fig. 12, the results of computation for streamlines are plotted with the value of cut as a parameter. $d\theta/d\Lambda$ was calculated along streamlines with the aid of the numerical differentiation formula for non-equidistant nodes [24] by using four neighbouring points and is shown as a function of Λ with the cut as a parameter in Fig. 13.

The above numerical computations were carried out of the flow of a supersonic jet into vacuum.

If the leading edge of the skimmer is located inside the region bounded by both the barrel shock and the Mach disk (see Fig. 14), the cut will not be affected by the change of inlet pressure as shown in Fig. 6. Bier and Schmidt [25] have reported a photographic study on the shape and size of the barrel shock and Mach disk. Their observed values on the Mach disk diameter, $y_M/2R^*$ and the maximum diameter of the barrel shock, $y_B/2R^*$ can be expressed as a function of the pressure ratio, p^0/p^1 by the following equations, over the range of p^0/p^1 of 10–10^3.

$$\frac{y_M}{2R^*} = 0{\cdot}252\left(\frac{p^0}{p'}\right)^{0\cdot598} \tag{50}$$

$$\frac{y_B}{2R^*} = 0{\cdot}316\left(\frac{p^0}{p^1}\right)^{0\cdot591}. \tag{51}$$

The relationship between the axial distance to the Mach disk and the pressure ratio has been given by Ashkenus and Sherman as follows [26]:

$$\frac{x_M}{R^*} = 1{\cdot}34\left(\frac{p^0}{p^1}\right)^{\frac{1}{2}}, 15 \leqslant \frac{p^0}{p^1} \leqslant 17000. \tag{52}$$

Under our experimental condition, these values were calculated from the above equations as shown in Table 1. Hence, the flow field of supersonic jet into vacuum can be directly used for calculating the mass transfer up to the skimmer, regardless of the change of jet boundary.

The calculated relationship between the cut and the nozzle to skimmer distance when the distance from the axis r/R^* is 2·0/0·3, is plotted in Fig. 6 for comparison with the experimental results. With the aid of the results for $d\theta/d\Lambda$, the integral, I was calculated for $r/R^* = 2{\cdot}0/0{\cdot}3$, by using Simpson integration formula.

As the first order approximation, both the mole fraction N_1, N_2 and the average mass of gas mixture $\bar{m}$ were assumed to be constant and equal to their values at the nozzle inlet. Then, the integral, I is given by

$$I = N_1^0 N_2^0 \int_0^{\Lambda} \left(\frac{T^0}{T}\right)^{\frac{1}{2}} M^{*2} \frac{d\theta}{d\Lambda} \bar{r}\, d\Lambda. \tag{53}$$

The results of calculation are shown in Fig. 7 by a solid line.

CONCLUSION

As indicated in Fig. 6, the experimental results on the relationship between the cut and the axial distance to the skimmer were in fairly good agreement with the results of calculation based on the flow pattern of axially symmetric supersonic jet into vacuum, which is computed by using the method of characteristics. This agreement has led to the conclusion that the flow properties up to the skimmer are unaffected by the jet boundary, that is, the leading edge of the skimmer is located inside the region bounded by both the barrel shock and the Mach disk under our experimental condition. The results on diffusive separation of hydrogen and nitrogen mixtures in an axially symmetric supersonic jet were also in fairly good agreement with the results of calculation by the proposed equations (14, 53) which were derived by taking account of the pressure diffusion in the jet.

ACKNOWLEDGEMENT

Some of the numerical computations were carried out by using the IBM 360/40 digital computer at the Chiyoda Chemical Engineering and Construction Company Ltd.

The participation of N. Sakai in the experiment is gratefully acknowledged. One of the authors (H. Mikami) was granted a scholarship from the Sakkokai Foundation and expresses his appreciation for the support.

REFERENCES

1. E. W. BECKER, W. BEYRICH, K. BIER, H. BURGHOFF and F. ZIGAN, Das Trenndüsenverfahren II, *Z. Naturf.* **12A**, 609 (1957).

Table 1. Experimental conditions

P^0	P^M	P^0/P^M	x_M/R^*	$y_M/2R^*$	$y\ /2R^*$	$y/2R^*$	$y_s/2R^*$
221·8	0·2	1109	46·4	16·7	19·9	1–10	$6\frac{2}{3}$
381·8	0·2	1909	58·6	23·1	27·5	1–10	$6\frac{2}{3}$
700·0	0·3	2333	77·4	26·0	30·9	1–10	$6\frac{2}{3}$

x_M, axial distance to the Mach disk; y_M, diameter of the Mach disk; y_B maximum diameter of barrel shock; x_s, axial distance to skimmer; y_s, diameter of skimmer.

2. G. NARDELLI and A. REPANAI, The physical principle of the method of the Trenndüse, II, *Energia Nucl., Milano* **5**, 247 (1958).
3. P. C. WATERMAN and S. A. STERN, Separation of gas mixture in a supersonic jet, *J. Chem. Phys.* **31**, 405 (1959).
4. R. R. CHOW, On the separation of binary gas mixture in an axisymmetric jet, University of California, HE-150-175 (1959).
5. F. ZIGAN, Gasdynamische Berechnung der Trenndüsenentmischung, *Z. Naturf.* **17A**, 772 (1962).
6. H. MIKAMI and Y. TAKASHIMA, Separation of isotope gas mixture in a supersonic jet, *Bull. Tokyo Inst. Technol.* No. 61, 67 (1964).
7. A. KOGAN, Separation of a gas mixture in curved supersonic flow, *Int. J. Heat Mass Transfer* **9**, 1 (1966).
8. F. S. SHERMAN, Hydrodynamical theory of diffusive separation of mixture in a free jet, *Physics Fluids* **8**, 773 (1965).
9. D. E. ROTHE, Electron beam studies of the diffusive separation of hellium–argon mixtures, *Physics Fluids* **9**, 1643 (1966).
10. N. ABUAF, J. B. ANDERSON, R. P. ANDRES, J. B. FENN and D. R. MILLER, Studies of low density supersonic jet, Project Squid Technical Report, PR-111-P (1966).
11. H. W. MEIVILLE and B. G. GOWENLOCK, *Experimental Method in Gas Reactions*, p. 223. MacMillan, London (1964).
12. H. MIKAMI, Y. ENDO and Y. TAKASHIMA, Analysis of two component gas mixture at low pressure by a thermistor-actuated thermal conductivity cell, *Bull. Tokyo Inst. Technol.* No. 69, 39 (1965).
13. H. MIKAMI, Y. ENDO and Y. TAKASHIMA, Heat transfer from a sphere to rarefied gas mixtures, *Int. J. Heat Mass Transfer* **9**, 1435 (1966).
14. H. MIKAMI and Y. TAKASHIMA, Critical mass flow of rarefied gas mixture through a slit nozzle, *Bull. Tokyo Inst. Technol.* No. 83, 103 (1968).
15. J. O. HIRSCHFELDER, C. O. CURTISS and R. B. BIRD, *Molecular Theory of Gases and Liquids*, p. 516. John Wiley, New York (1960).
16. J. O. HIRSCHFELDER, C. O. CURTISS and R. B. BIRD, *Molecular Theory of Gases and Liquids*, p. 539. John Wiley, New York (1960).
17. J. O. HIRSCHFELDER, C. O. CURTISS and R. B. BIRD, *Molecular Theory of Gases and Liquids*, p. 1164. John Wiley, New York (1960).
18. L. WALDMANN, Transporterscheinungen in Gasen von mittlerem Druck, *Handb. Phys.* **12**, 429 (1958).
19. H. W. LIEPMANN and A. ROSHKO, *Elements of Gasdynamics*, p. 292. John Wiley, New York (1957).
20. O. M. BELOTSERKOVSKII and P. I. CHUSHKIN, The numerical solution of problems in gas dynamics, in *Basic Developments in Fluid Dynamics*, edited by M. HOLT, p. 1. Academic Press, New York (1965).
21. O. N. KATSKOVA and Y. D. SHMYGLEVSKII, Axisymmetric supersonic flow of a freely expanding gas with plane transition surface, *Sb. Vych. Mat.* **2**, 45 (1957).
22. O. N. KATSKOVA, On axisymmetric supersonic expansion of a real gas, *Zh. Vychis. Mat. Mat. Fiz.* **1**, 301 (1961).
23. C. J. WANG and J. B. PETERSON, Spreading of supersonic jets from axially symmetric nozzles, *Jet. Propul.* **58**, 321 (1958).
24. I. S. BEREZIN and N. P. ZHIDKOV, *Computing Methods*, Vol. 1, p. 196. Pergamon Press, Oxford (1965).
25. K. BIER and B. SCHMIDT, Zur Form der Verdichtungsstösse in frei expandierenden Gasstrahlen, *Z. Angew. Math. Phys.* **13**, 493 (1961).
26. H. ASHKENAS and F. S. SHERMAN, The structure and utilization of supersonic free jet in low density wind tunnels, in *Rarefied Gas Dynamics*, edited by J. H. LEEUW, Vol. 2, p. 91. Academic Press, New York (1966).

Résumé—On étudie la séparation d'un mélange gazeux dans un jet supersonique à symétrie axiale.

Le jet supersonique est séparé en un écoulement phériphérique et un écoulement central par un écrémeur et l'on obtient le flux de diffusion totale du constituant le plus léger dans l'écoulement périphérique. Les résultats expérimentaux sont présentés pour le mélange gazeux binaire d'hydrogène et d'azote.

On propose une équation approchée qui donne le flux di diffusion en fonction du partage et du nombre de Mach. Les résultats expérimentaux étaient en très bon accord avec les résultats du calcul par l'équation proposée.

Zusammenfassung—Es Wird die Trennung eines Gasgemisches in einem axialsymmetrischen Überschallstrom untersucht. Der Überschallstrom wird durch ein Rührblech in die Rand- und die Kernströmung aufgeteilt und damit der gesamte Diffusionsstrom der leichteren Komponente in die Randströmung erhalten.

Die experimentellen Ergebnisse werden für das Zweistoffgemisch Wasstestoff-Stickstoff dargestellt.

Eine Näherungsgleichung wird vorgeschlagen, die den Diffusionsstrom als Funktion des Schnittes und der Machzahl wiedergibt. Die experimentellen Ergebnisse standen in ziemlich guter Übereinstimmung mit den Rechenergebnissen aus der vorgeschlagenen Gleichung.

Аннотация—Изучается распределение газовой смеси в осесимметричной сверхзвуковой струе.

С помощью сепаратора сверхзвуковая струя разделена на два потока. Получен суммарный диффузионный поток более легкого компонента в периферийном потоке. Представлены экспериментальные результаты по бинарной газовой смеси водорода и азота.

Предлагается приближенное уравнение, в котором диффузионный поток есть функция угла наклона и числа Маха. Экспериментальные данные хорошо согласуются с результатами, полученными по предложенному уравнению.